Available online at www.sciencedirect.com
SCIENCE DIRECT®
PERGAMON
Solid State Communications 127 (2003) 483–487
solid state communications
www.elsevier.com/locate/ssc

Atomic topology and radial distribution functions of *a*-SiN_x alloys: ab initio simulations

Fernando Alvarez, Ariel A. Valladares*

Instituto de Investigaciones en Materiales-UNAM, Materia Condensada, Ciudad Universitaria, Circuito Exterior, Apartado Postal 70-360, México D.F., 04510, Mexico

Received 23 November 2002; accepted 4 June 2003 by M. Cardona

Abstract

Random structures of amorphous silicon–nitrogen alloys, *a*-SiN_x, are obtained for several values of x from 0 to the nearly stoichiometric composition of $x = 1.29$, using a new ab initio thermal procedure based on a Harris-functional code and periodically continued cells with 64 atoms. Partial radial features are reported with no experimental counterparts for comparison, whereas the total radial distribution functions agree very well with the few existing experiments. Our average coordination numbers also agree very well with experiment. These results, being predictive, may stimulate further experimental and theoretical studies.

PACS: 71.23.Cq; 71.15.Pd; 71.55.Jv

Keywords: A. Disordered systems; A. Semiconductors; C. Impuritites in semiconductors

The simulational generation of atomic random networks of covalent materials has encountered serious obstacles hindering progress in the understanding of the atomic, electronic and optical properties of amorphous semiconductors. Classical potentials and parameterized quantum approaches carry the stigma of non-transferability, although lately promising developments have taken place along those lines. Recently [1], we developed a thermal procedure to generate structures of pure and hydrogenated amorphous silicon using an ab initio Harris-functional-based code on periodic supercells with 64 silicon atoms plus hydrogens that diffuse within the cells. This procedure was then applied to amorphous carbon, germanium and silicon nitride to investigate its general applicability [2], and we now apply it here to the amorphous alloys of silicon–nitrogen to test the predictive powers of our thermal procedure. These are the first ab initio thermally generated amorphous networks of *a*-SiN_x; the content x is in the range $0 \leq x \leq 1.29$ where $x = y/(64 - y)$ and y is the number of nitrogen atoms.

The properties of amorphous silicon–nitrogen alloys have attracted a great deal of attention in recent years; *a*-SiN_x have electrical, optical and mechanical features useful in a variety of industrial applications and the strength of their bonding makes them the prototype of covalent materials. Their optical gaps depend strongly on the nitrogen content x for $0 \leq x \leq 1.33$ so they can be tuned to fit specific needs in solar cells, and their total and partial radial distribution functions (RDFs) are practically unknown, except for the stoichiometric content. Some semiempirical studies have been done on their electronic structure and optical gaps and a first-principles approach has been used on an ad hoc-generated amorphous structure. Therefore, any ab initio approach that adequately generates, describes and predicts features of *a*-SiN_x may have a wider applicability for dealing with other covalently bonded amorphous solids; in particular, systems like *a*-GeN_x should be amenable to this approach [3].

The experimental and theoretical activity prior to 1990 is well documented in a paper by Robertson [4]. Bethe lattice simulations have been carried out using semiempirical parameters [5,6], whereas Ordejón and Ynduráin [7] do

* Corresponding author. Tel./fax: +52-55-5622-4636.
E-mail address: valladar@servidor.unam.mx (A.A. Valladares).

0038-1098/03/$ - see front matter © 2003 Elsevier Ltd. All rights reserved.
doi:10.1016/S0038-1098(03)00483-6

non-parameterized calculations of a-SiN_x where the equilibrium positions of Si and N atoms in clusters are ported to the alloy network constructed ad hoc. Although they obtain a wealth of information, tetrahedral coordination of the silicon atoms and threefold planar coordination of the nitrogen atoms is *assumed* throughout, with interatomic distances of 2.33 Å for Si–Si and 1.74–1.76 Å for Si–N. A general characteristic of all these calculations/simulations is that no RDFs are reported and that gap states, when considered, are introduced either by hand progressively replacing Si by N, or by algorithms that generate the random networks. Recent Tersoff-like classical simulations by de Brito et al. [8] produced total RDFs and average coordination numbers, $\langle cn \rangle$, that are the subject of comparison with ours.

Experimentally, as early as 1976 Voskoboynikov et al. [9] studied some RDFs and optical gaps of silicon-rich silicon–nitrogen films as a function of the gas ratio. They observed that the gaps increased as a function of the nitrogen content; the films seemed to contain hydrogen and large clusters of silicon. However, reliable experimental RDFs are scarce [10] and, apparently, only total ones for the stoichiometric amorphous composition exist [11].

It is clear that the atomic topology determines the electronic structure and optical properties of the amorphous samples, and therefore any understanding of the RDFs and the atomic distribution in the random networks is relevant in the electrical and optical characterization of these materials. In what follows we report the generation of random networks for amorphous silicon nitrogen alloys that leads to RDFs and average coordination numbers in good agreement with the existing experimental results, and we obtain atomic structures for a variety of nitrogen contents. Unlike other simulations, electronic gap states are found in these structures.

Twenty-six amorphous samples of a-SiN_x were generated with FASTSTRUCTURE [12], a DFT code based on the Harris functional. The optimization techniques use a fast force generator to allow simulated annealing/molecular dynamics studies with quantum force calculations [13]. The LDA parameterization invoked is that due to Vosko, Wilk and Nusair [14]. An all electron calculation is carried out, and a minimal basis set of atomic orbitals was chosen with a cutoff radius of 5 Å for the amorphization and 3 Å for the optimization. The physical masses of nitrogen and silicon are used throughout and this allows us to see realistic randomizing processes of the atoms during the amorphization of the supercell. Finally, the forces are calculated using rigorous formal derivatives of the expression obtained for the energy [15].

In order to test the adequacy of the calculations carried out with FASTSTRUCTURE we used it to obtain the size of the crystalline cell of β-Si_3N_4 that minimizes the energy at the Γ-point. The experimental crystalline volume is 145.920 $Å^3$[16] and the calculated volumen is 146.797 $Å^3$; a deviation of 0.6%. Also, work by Polatoglou and Methfessel [17] has established that the Harris functional approximation adequately describes many properties of both pure silicon and a highly ionic system like NaCl: elastic constants and phonon frequencies of silicon; the cohesive energy, the lattice constants and the bulk modulus of NaCl. Therefore we feel that their results indicate that the use of the Harris approximation in the ionic SiN alloys is justified. Finally, the agreement of the total RDF for the almost stoichiometric amorphous sample of SiN and of the composition of its second peak [2] with experiment, and the agreement between the coordination numbers predicted herein and experimental results, Fig. 2, make us cautiously optimistic about our approach to generate random networks of silicon–nitrogen alloys. Our calculated optical gaps for these alloys are also in reasonable agreement with experiment [18].

It has become increasingly clear that quenching from a melt generates an excess of bond defects, both dangling and floating. Therefore, we took a different path [1,2]. We amorphisized the crystalline diamond structures with a total of 64 atoms ($(64 - y)$ silicons and y substitutional nitrogens) in the cell by slowly heating it, linearly, from room temperature to just *below* the corresponding melting point for each x, and then slowly cooling it to 0 K. To determine the melting temperatures for each x we linearly interpolated between the pure silicon and the stoichiometric compound ($x = 4/3 = 1.33$), values and then remained below them (Table 1). Since the time step was the same for all runs, 6 fs, and the melting temperatures increased with x, the heating/cooling rate varied from 2.30×10^{15} K/s for pure silicon, to 3.11×10^{15} K/s for $x = 1.29$. The atoms were allowed to move within each cell whose volume was determined by the corresponding density and content, Table 1. The densities were taken from the experimental results of Guraya *et al.*[10]. Once this first stage was completed, we subjected each cell to annealing cycles with intermediate quenching processes. Finally the samples were geometry-optimized to make sure the final structures were those of a local energy minimum.

Table 1
Contents, amorphization temperatures and densities for a-SiN_x

Sample	x	Amorphization temp. (K)	Density (g/cc)
$Si_{64}N_0$	0.000	1680	2.329
$Si_{59}N_5$	0.085	1747	2.435
$Si_{54}N_{10}$	0.185	1814	2.512
$Si_{49}N_{15}$	0.306	1881	2.600
$Si_{44}N_{20}$	0.455	1948	2.694
$Si_{39}N_{25}$	0.641	2015	2.803
$Si_{34}N_{30}$	0.882	2082	2.931
$Si_{33}N_{31}$	0.939	2095	2.957
$Si_{32}N_{32}$	1.000	2108	2.988
$Si_{31}N_{33}$	1.065	2122	3.017
$Si_{30}N_{34}$	1.133	2136	3.048
$Si_{29}N_{35}$	1.207	2149	3.081
$Si_{28}N_{36}$	1.286	2162	3.115

It should be kept in mind that our objective is always to generate representative amorphous structures of a-SiN_x within our approximations, and not, in any way, to mimic the experimental processes used to produce these alloys.

We performed two runs for each x value and from $x = 0.882$ (a-$Si_{34}N_{30}$) on, the nitrogens were increased one at a time to be able to map the interesting processes that occur for these contents, (percolation of the Si–Si bonds, widening of the optical gaps, etc). Once the atomic structures were obtained, we calculated the corresponding total and partial RDFs for each of the 26 runs and averaged them by corresponding pairs. Of those 13 averaged plots we are reporting here total and partial RDFs for pure silicon, for the almost stoichiometric sample, a-$Si_{28}N_{36}$, $x = 1.29$, and two intermediate ones: a-$Si_{44}N_{20}$, $x = 0.46$ and a-$Si_{32}N_{32}$, $x = 1.00$. The results for the pure amorphous silicon sample are given in Fig. 1a where the upper and lower bounds of the available experimental data [1,2] are included; the agreement is good since our RDF falls within these bounds and the four experimental peaks are correctly reproduced by our simulations. Fig. 1b–d show the variation of the partial RDFs for Si–Si, Si–N and N–N as a function of content and their contribution to the total RDF. In Fig. 1d the composition of the second peak of the total RDF for the nearly a-Si_3N_4 can be observed and it agrees completely with experiment [19,2], since it is formed by the average second-neighbor $\langle 2n \rangle$ contributions of mainly the N–N and Si–Si partials and to a lesser extent by the Si–N partial. We predict that the third peak is essentially due to the Si–N partial with a small contribution from the N–N partial; experimental results are lacking.

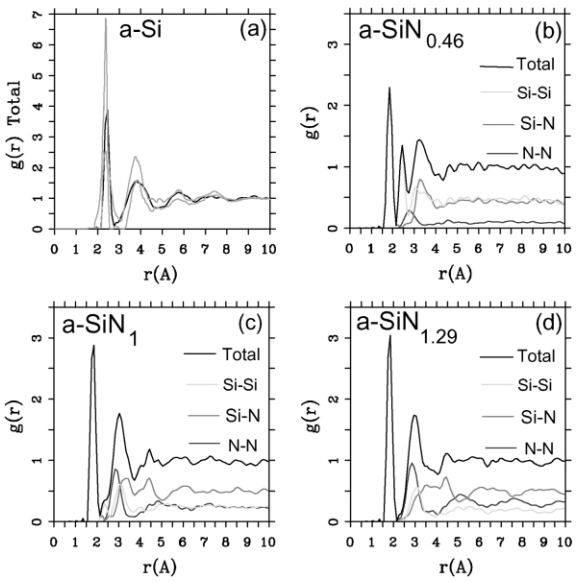

Fig. 1. Total and partial RDFs for (a) pure silicon; the light curves are the upper and lower experimental bounds [1,2]; (b) a-$Si_{44}N_{20}$, $x = 0.46$; (c) a-$Si_{32}N_{32}$, $x = 1.00$; and (d) the nearly stoichiometric sample a-$Si_{28}N_{36}$, $x = 1.29$.

Fig. 1 show that as the nitrogen content increases the first peak of the total RDF (1.85 Å), which is due to the Si–N average nearest-neighbor ($\langle nn \rangle$ contributions), increases systematically and the $\langle nn \rangle$ Si–Si peak (2.45 Å) decreases systematically. The third peak moves toward low r as x increases since the N–N contribution becomes more predominant at high content (3.25–2.95 Å). In our structures there are no $\langle nn \rangle$ nitrogens since the content is below stoichiometry and nitrogens have a marked tendency to bind to silicons, even though, for $x > 1$ there are $\langle nn \rangle$ nitrogens in the original crystalline cells. For the nearly stoichiometric sample, $x = 1.29$, the Si–Si $\langle nn \rangle$ contribution to the total RDF has practically disappeared and this implies that there is a nitrogen atom between every pair of silicons. This is borne out by the results presented in Fig. 2 where a study of the average coordination numbers $\langle cn \rangle$ in the 13 random networks is depicted. The following cutoff radii were used: Si–Si, 2.55 Å; N–N, 3.35 Å; and Si–N, 2.15 Å, which are the positions of the minima after the first peaks of the corresponding partials. Fig. 2a shows the results of our simulations where it can be seen that the N–N plot flattens for $x \approx 1.1$, the percolation threshold of Si–Si bonds [20]; the Si–Si $\langle nn \rangle$ go from 4 to practically 0. The Si–N graph refers to the $\langle nn \rangle$ nitrogens around the silicon atoms and varies from 0 to 4, whereas the N–Si refers to the $\langle nn \rangle$ silicons around nitrogens and indicates that nitrogens immediately surround themselves with practically 3 Si, saturating its valence. The crossing of the Si–Si and Si–N plots at $x \approx 0.7$, is in agreement with experiment (Davis et al. [10]). There is a crossing of the Si–Si, N–Si and N–N plots at $x \approx 0.3$ and a crossing of N–Si and Si–N at $x \approx 1.0$. These crossings have been observed experimentally for *hydrogenated* alloys by Guraya et al.[10], Fig. 2b; however, due to the presence of hydrogen a curvature appears in the $\langle cn \rangle$ for Si–Si, Si–N and N–Si. In order to compare our results to this experiment we did the following: we carried out the sum of N–H and N–Si from the experiment to obtain the total number of atoms that surround a N, N–*, and plotted it along with our N–Si; we also did the sum of the experimental Si–N, Si–Si and Si–H, the total number of atoms that surround a Si, Si–*, and plotted that along with our sum of Si–N plus Si–Si. This is presented in Fig. 2c. It is clear that our predictions closely agree with the integrated experimental results. The discrepancies are most likely due to the presence of dangling and floating bonds.

In Fig. 3 we present a comparison of our ab initio results and experiment and also, a comparison of the classical Monte Carlo simulations of de Brito et al. [8] and experiment. de Brito et al. used empirical potentials developed a la Tersoff for the interactions between Si and N. The agreements and discrepancies can be appreciated.

In conclusion we have applied our recently developed thermal process to a-SiN_x ($0 \leq x \leq 1.29$) and have generated radial distribution functions that are in agreement with existing experimental results and random atomic structures where the simulated average coordination

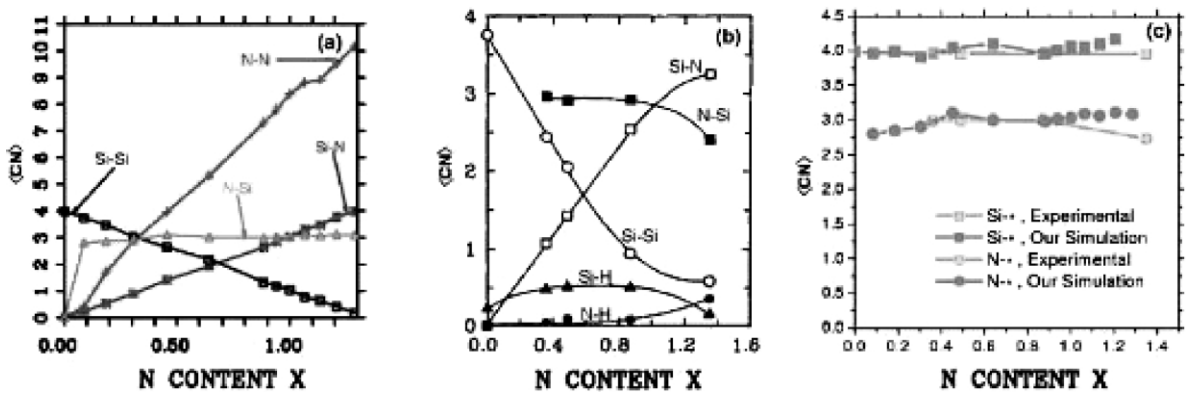

Fig. 2. Average coordination numbers $\langle cn \rangle$ as a function of x. (a) Our results. (b) Experimental results for hydrogenated alloys from Guraya et al. (c) Comparison of the integrated results (see text). Lines are drawn as guides to the eye.

numbers and the experimental ones coincide. Total RDFs agree very well with experiment where available, and partial RDFs show that the Si–Si $\langle nn \rangle$ peak disappears as nitrogen increases indicating a tendency to form 6-atom arrangements as the content x approaches the stoichiometric value. Experiment shows that for a-Si_3N_4, Si and N form closed rings, Si–N–Si–N–Si–N, typical of the crystalline Si_3N_4 structures. The growth of the simulated Si–N peak as nitrogen increases bears out this behavior. No nitrogen–nitrogen bonds, including molecules, are observed in the final structures even though for $x > 1$ the starting diamond structure *does* contain nitrogens next to one another.

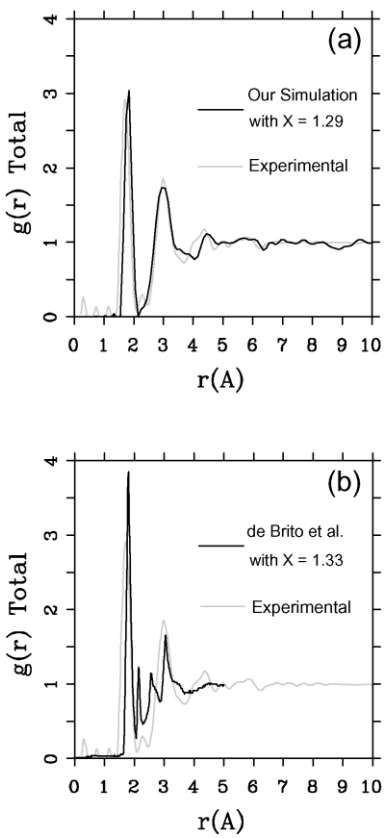

Fig. 3. Results for the stoichiometric sample. (a) Comparison of our simulations and experiment [11]. (b) Comparison of de Brito's simulations and experiment [11].

For $x \approx 1.1$ the effects of the percolation threshold of the Si–Si bonds is observed in the N–N $\langle 2n \rangle$. For $x \approx 0.7$ the Si–Si and Si–N neighbors are practically the same, as found experimentally. Also, Si–Si, N–Si an N–N are practically the same for $x \approx 0.3$ as are Si–N and N–Si for $x \approx 1.0$. The integrated experimental results and our simulation agree. The first prominent peak in the total RDF of the nearly stoichiometric sample is due to Si–N and an analysis of the second peak indicates that N–N, Si–Si and Si–N contribute to it, in agreement with experiment. The third peak is mainly due to the Si–N, with a small contribution from the N–N; no experimental results exist for comparison. Our approach, being ab initio, is of wider applicability than classical or semiempirical ones and should be relevant for the understanding of the physics of amorphous covalent materials.

Acknowledgements

A.A.V. thanks DGAPA-UNAM for financing projects IN101798 and IN100500. F.A. thanks CONACyT for supporting his PhD studies. This work was done on an Origin 2000 computer provided by DGSCA, UNAM.

References

[1] A.A. Valladares, F. Alvarez, Z. Liu, J. Stitch, J. Harris, Eur. Phys. J. B 22 (2001) 443.
[2] F. Alvare, C.C. Díaz, A.A. Valladares, R.M. Valladares, Phys. Rev. B 65 (2002) 113108. F. Alvarez, A.A. Valladares, Rev. Mex. Fís. 48 (2002) 528.

[3] P.P.M. Venezuela, A. Fazzio, Phys. Rev. Lett. 77 (1996) 546.
[4] J. Robertson, Philos. Mag. B 63 (1991) 47.
[5] L. Martín-Moreno, E. Martínez, J.A. Vergés, F. Yndurain, Phys. Rev. B 35 (1987) 9689.
[6] E. San-Fabián, E. Louis, L. Martín-Moreno, J.A. Vergés, Phys. Rev. B 39 (1989) 1844.
[7] P. Ordejón, F. Ynduráin, J. Non-Cryst. Solids 137 and 138 (1991) 891.
[8] F. de Brito Mota, J.F. Justo, A. Fazzio, Phys. Rev. B 58 (1998) 8323. F. de Brito Mota, J.F. Justo, A. Fazzio, Int. J. Quantum Chem. 70 (1998) 973. F. deBrito Mota, J.F. Justo, A. Fazzio, J. Appl. Phys. 86 (1999) 1843. J.F. Justo, F. deBrito Mota, A. Fazzio, Multiscale modelling of materials, Symposium Mater. Res. Soc. (1999) 555.
[9] V. Voskoboynikov, V.A. Gritsenko, N.D. Dikovskaya, B.N. Saitsev, K.P. Mogilnicov, V.M. Osadchii, S.P. Sinitsa, F.L. Edelman, Thin Solid Films 32 (1976) 339.
[10] S. Hasegawa, M. Matuura, Y. Kurata, Appl. Phys. Lett. 49 (1986) 1272. E.A. Davis, N. Piggins, S.C. Bayliss, J. Phys. C 20 (1987) 4415. M.M. Guraya, H. Ascolani, G. Zampieri, J.I. Cisneros, J.H. Dias da Silva, M.P. Cantão, Phys. Rev. B 42 (1990) 5677. G. Santana, A. Morales-Acevedo, Solar Energy Mater. Solar Cells 60 (2000) 135.
[11] T. Aiyama, T. Fukunaga, K. Niihara, T. Hirai, Suzuki K, J. Non-Cryst. Solids 33 (1979) 131.
[12] FASTSTRUCTURE_SIMANN, User Guide, Release 4.0.0 (San Diego, Molecular Simulations, Inc., September 1996).
[13] X.-P. Li, J. Andzelm, J. Harris, A.M. Chaka, in: Ziegler (Ed.), Anaheim Symposium, American Chemical Society, 1996, Chapter 26.
[14] S.H. Vosko, L. Wilk, M. Nusair, Can. J. Phys. 58 (1980) 1200.
[15] Z. Lin, J. Harris, Phys. Condens. Matter 4 (1992) 1055.
[16] S. Wild, P. Grieveson, K.H. Jack, The crystal structure of alpha and beta silicon and germanium nitrides, Special Ceramics (1972) 385.
[17] H.M. Polatoglou, M. Methfessel, Phys. Rev. B 37 (1988) 10403. H.M. Polatoglou, M. Methfessel, Phys. Rev. B 41 (1990) 5898.
[18] F. Alvarez, A.A. Valladares, Appl. Phys. Lett. 80 (2002) 58.
[19] M. Misawa, T. Fukunaga, K. Niihara, T. Hirai, K. Susuki, J. Non-Cryst. Solids 34 (1979) 313.
[20] E. Martínez, F. Ynduráin, Phys. Rev. B 24 (1981) 5718.